Acta Polytechnica CTU Proceedings **49**:41–47, 2024
https://doi.org/10.14311/APP.2024.49.0041

Published by the Czech Technical University in Prague

NUMERICAL MODELING OF CONCRETE BEAMS SUBJECTED TO PARTIAL WETTING AND DRYING CYCLES

Štěpán Krátký*, Petr Havlásek

Czech Technical University in Prague, Faculty of Civil Engineering, Department of Mechanics, Thákurova 7, 166 29 Prague, Czech Republic

* corresponding author: 1kratkystepan@gmail.com

Abstract. Concrete structures are commonly subjected to cycles of wetting and drying, which can have a significant impact on their behavior. However, experimental data on the effects of wetting and drying on concrete beams are scarce. This study presents the results of a 4-year experimental program on 2.5 m span concrete beams with heights of 100 mm, 150 mm, and 200 mm subjected to one-sided wetting and drying cycles. Vertical deflection of the beams was monitored throughout the experiment, and moisture mass balance was measured on companion specimens.

The behavior of the specimens was experimentally assessed, and subsequently numerical models using coupled hygromechanical finite element simulations were developed. The purpose of the simulations was to verify the prediction capabilities of the established constitutive models for moisture transport and creep and shrinkage of concrete and, if needed, to propose necessary corrections to the constitutive models.

Keywords: Concrete, creep, shrinkage, drying, cyclic temperature, modeling.

1. Introduction

Although the effects of moisture on the time-dependent behavior of concrete have been studied for decades, existing data are typically limited to cases where the concrete element is exposed to constant air humidity uniformly across the whole surface [1–4]. However, in reality, structural members are frequently subjected to cycles of highly variable ambient conditions. Data are scarce for cycles of contact with water and subsequent exposure to air, and/or the influence of sunlight [5–7], and focus primarily on axial strain.

In 2019, an extensive experimental campaign was initiated at the CTU in Prague to study the time-dependent behavior of structural concrete exposed to drying conditions [8]. All samples were prepared from a single concrete batch and cured for one month. The key component was a set of simply supported plain concrete beams of various sizes $L = 1.75$–3.0 m, $h = 0.05$–0.2 m and sealing setups which influenced not only the drying rate, and the development of vertical deflection, but also the degree of internal restraint and thus the extent of damage.

A set of spare specimens was used to investigate the effects of one-sided wetting and drying cycles. Within the experiment, deflection of simply supported beams with heights of 100, 150, and 200 mm and a span of 2.5 m was measured. After one year of drying, beams were placed inside a tank and repeatedly partially immersed (≈ 25 mm). The measurement results revealed that the response in the individual cycles varies depending on the number of previous cycles and the moisture content of the specimens. The data suggest that the members may undergo irreversible changes.

This paper summarizes the methods and results of the first author's master's thesis [9]. The first part describes the computational models, the second part presents the results of the blind prediction and the constitutive models employed, which aimed to understand the modeled problem and assess the predictive capabilities of the material models. The final part shows selected results from the refined simulations, which were designed to replicate the course of the experiment more accurately, and to identify potential causes of the variable behavior of the specimens between individual cycles.

2. Numerical modeling

A weakly coupled computational approach was used to model the moisture-induced structural response. Two sets of computational models were created for simulations:

(1.) Beams with different heights (as shown in Figures 1 and 2),

(2.) companion specimens used to measure the moisture content that did not consider the structural response.

The OOFEM finite element solver [10] was used to run all numerical simulations.

A finite element mesh of the beams and accompanying specimens represents a symmetric quarter of the real specimen. Suitable boundary conditions are defined on the symmetry planes to impose symmetric behavior (zero moisture flux and zero out-of-plane displacement). The mesh is finer near the surfaces, with an edge element thickness of 2 mm, to improve the convergence of computation and to capture the

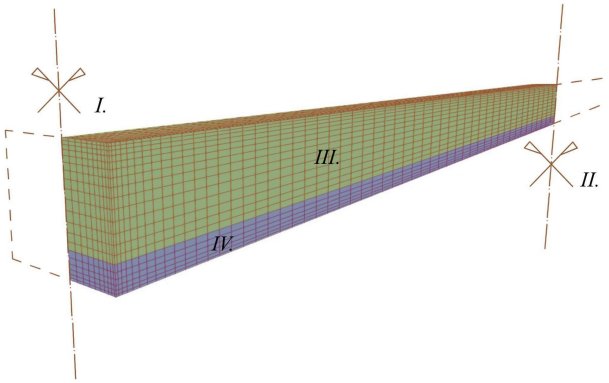

(I.) Longitudinal plane of symmetry,
(II.) mid-span plane of symmetry,
(III.) continuously exposed area to air,
(IV.) cyclically submerged area.

Figure 1. Outline of the moisture transport (MT) model.

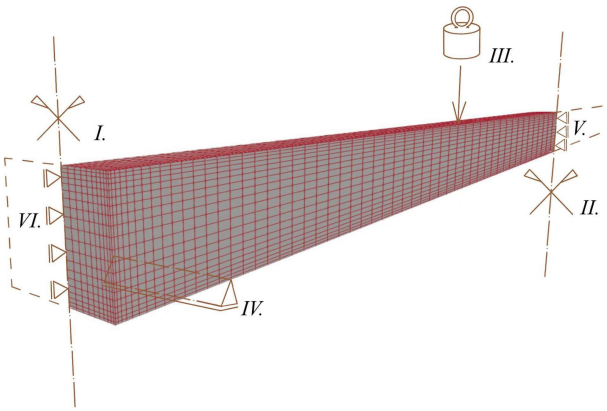

(I.) Longitudinal plane of symmetry,
(II.) mid-span plane of symmetry,
(III.) auxiliary weight,
(IV.) pin support,
(V.) mid-span symmetry BC,
(VI.) longitudinal symmetry BC.

Figure 2. Outline of the mechanical response (SM) model.

expected strong nonlinear behavior of the moisture profile.

For numerical simulations, the primary time step length is chosen to be 0.5 days. To improve convergence at the beginning of the simulations and humidity cycles, the step length is substantially reduced to 10^{-4} days and then gradually increased with a geometric progression until it reaches the primary step length.

The evolution of ambient humidity is shown in Figure 3. Experimental data indicate that the rate of wetting is much higher than the rate of drying. To realistically capture this phenomenon, during wetting cycles, the surface factor f, which appears in the mixed boundary condition for moisture transfer, is set to a large number to effectively become a Dirichlet boundary condition. Otherwise, its value is set to 1 mm/day.

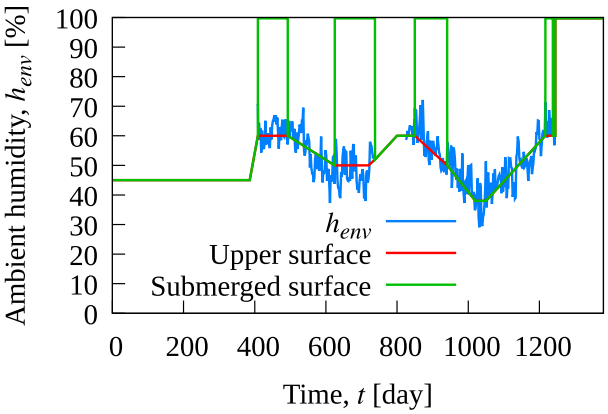

Figure 3. Measured (blue) and simplified (red) evolution of ambient relative humidity, wetting cycles assigned to the immersed portion are shown in green.

3. Blind prediction

3.1. Constitutive models

In the blind prediction, the transport of moisture in concrete is described by a widely accepted model proposed by Bažant and Najjar [11] that assumes a linear sorption isotherm. In the present case, the moisture capacity is set to 130 kg m^{-3} (see Figure 4). With this assumption, the governing equation for a diffusion of water vapor simplifies to:

$$\frac{\partial h}{\partial t} = \nabla \cdot (C(h) \nabla h)\,, \qquad (1)$$

where

$\nabla\cdot$ is the divergence operator,

∇h is the gradient of relative humidity,

$C(h)$ is the humidity-dependent diffusivity.

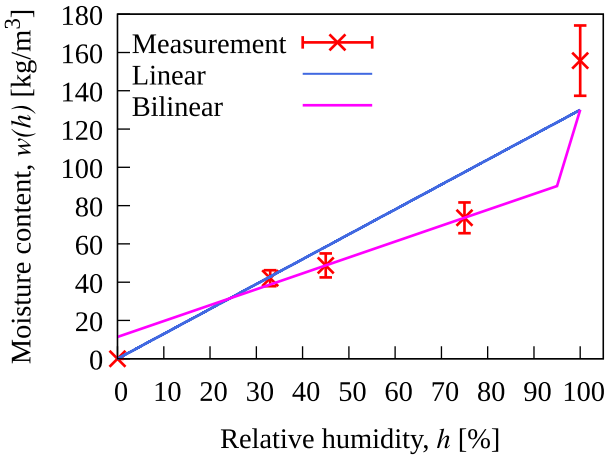

Figure 4. Experimental data of the sorption isotherm and its linear and bilinear approximation used in the blind prediction and calibrated model, respectively.

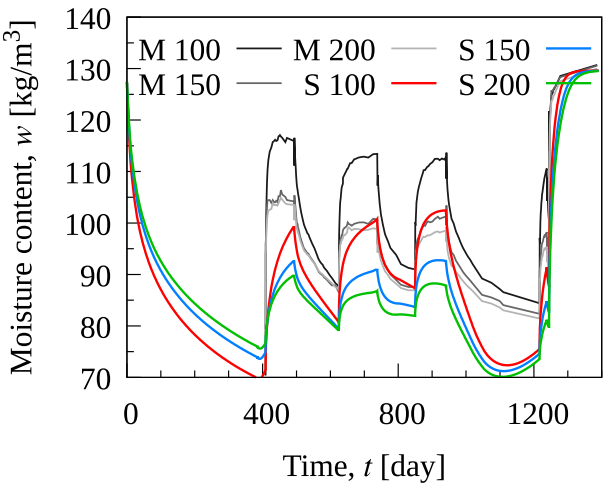

FIGURE 5. Evolution of the average moisture content in the companion specimens (M – measurement in grey scale) and in the blind prediction (S – simulation in colors). The numbers in the legend denote the height of the specimens. The time t corresponds to the material age.

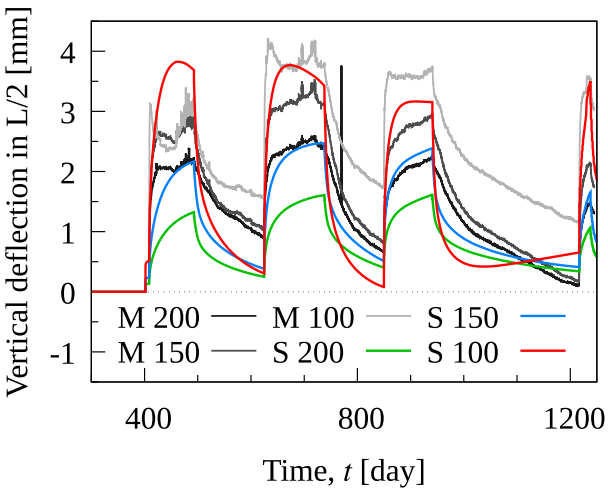

FIGURE 6. Evolution of vertical mid-span deflection of beams in the experiment (grey scale) and in the blind prediction (colors). The numbers in the legend denote the height of the beams. The time t corresponds to the material age.

The model parameters are prescribed according to the recommended values in the *fib* Model Code 2010 [12] from the compressive strength of concrete.

The mechanical behavior of concrete is described by a Microprestress-solidification (MPS) theory [13] modified to diminish the size-effect on drying shrinkage [14]. Under hygrally sealed conditions and constant room temperature, this model reduces to the basic creep compliance function of the B3 model [15] whose parameters $q_1 - q_4$ were estimated from the composition of the concrete mixture.

Changes in relative humidity give rise not only to volume changes (shrinkage/swelling) but also to further creep (Pickett effect). This additional creep is primarily controlled by the parameter k_3 [14]. Shrinkage strain and relative humidity are linearly linked via their rates:

$$\dot{\varepsilon}_{\mathrm{sh}} = k_{\mathrm{sh}} \dot{h}, \tag{2}$$

where k_{sh} is a material parameter usually treated as a humidity- and age-independent constant. In the initial blind prediction, the parameters of the MPS model k_3 and k_{sh} were calibrated to match the evolution of shrinkage and drying creep given by the (cross-sectional) B3 model.

3.2. Evolution of moisture content

Figure 5 shows the measured and predicted evolution of the average moisture content related to the total volume of the individual specimens. Since the initial state is not known exactly, the vertical offset of the experimental measurements is determined by setting the last part of this evolution (which corresponded to a fully submerged condition and almost saturated state) to 130 kg m^{-3}. Comparison of the blind prediction to the experimental data demonstrates that even though the drying rate is captured quite accurately, the rate of moisture intake during the wetting stages is significantly underestimated. Additionally, the moisture balance in the individual drying and wetting cycles is less than the measured values. This implies that the moisture capacity and/or the portion of the specimen that experiences wetting is underestimated. The latter statement is supported by the distribution of relative humidity over the cross section (not presented here), which shows that the fully saturated state is only at the boundary. Only 2 mm from the surface, the humidity drops to 97.9 %.

3.3. Mechanical response

Figure 6 presents the evolution of the mid-span deflection of the concrete beams subject to drying and wetting cycles. The readings are zeroed with respect to the instant just before applying the self-weight whose contribution to the overall deflection is negligible compared to the swelling- and shrinkage- induced strains. The positive sign corresponds to downward deflection. In the figure, the experimental measurements (series M) on the three beams with different heights of 100, 150, and 200 mm are shown in gray scale while the blind prediction of the FEM simulation (series S) is drawn in colors.

Considering the fact that the presented results are truly the results of a blind prediction, the agreement with the experimental data can be considered promising. During wetting cycles, graphical postprocessing revealed that the evolution of the moisture field in the lower part of the cross section is very similar for all three cross-section heights, which in turn implies that the swelling action is also similar.

The computed data series are in correct order and correspond with the experiment; the highest deflection

is observed in the specimen with the smallest height of the cross section (and thus bending stiffness) and vice versa. A stiffer cross section providing stronger internal restraint produces higher magnitudes of self-equilibrated internal stresses.

Since the moisture intake rate was underestimated in the transport model, the mechanical response is also lagging behind the experiment. However, during drying, the computed deflection tends to return faster to the initial position than what is observed in the experiment. The contribution of creep to the total deflection is rather small, as demonstrated by the computed deflections at the end of the drying cycle.

Graphical post-processing of the mechanical analysis also revealed that shortly after the onset of wetting or drying, tensile stresses that exceed the tensile strength develop. The origin of these stresses stems from a highly variable field of eigenstrains produced by swelling or shrinkage which need to be balanced by a self-equilibrated normal stresses. The results obtained from an additional analysis in which tensile cracking was introduced using the concept of damage mechanics have shown that cracking leads to an increase in irreversible deformation at the end of the drying cycles.

4. Improved modeling approach

The results of the blind prediction with Bažant-Najjar model have shown that this approach does not give a realistic response when modeling drying and wetting cycles in which the concrete is in direct contact with the water. The primary reason for insufficient variation in moisture content is the presence of a linear sorption isotherm, which might be sufficient when modeling monotonous drying. To alleviate this problem, a nonlinear isotherm with a higher moisture capacity needs to be considered when approaching free saturation. However, the combination of Bažant-Najjar model with nonlinear isotherm would have led to an unrealistic response. For this reason, a more advanced constitutive model proposed by Künzel [16] is adopted instead. This model was developed and validated for transport tasks similar to those in the case of the experiment presented.

With the assumption of constant temperature and zero moisture sink, the moisture balance equation reads:

$$\frac{\partial w}{\partial h}\cdot\frac{\partial h}{\partial t}=\nabla\cdot\left[\left(D_w\frac{\partial w}{\partial h}+\delta_p p_{\mathrm{sat}}\right)\nabla h\right], \qquad (3)$$

where

w is the moisture content,

D_w is the capillary transport coefficient [$\mathrm{m^2\,s^{-1}}$],

δ_p is the water vapor permeability,

p_{sat} is the saturation vapor pressure.

The expression for the transport coefficient that is dominant at higher values of relative humidity – and so in the present case – reads:

$$D_w=3.8\left(\frac{A}{w_f}\right)^2 1000^{\frac{w}{w_f}-1}, \qquad (4)$$

where

A is the water absorption coefficient, with typical values ranging between 0.1–1.0 $\mathrm{kg\,m^{-2}\,day^{-0.5}}$,

w_f is the moisture content at free saturation.

The water vapor permeability of the building material that becomes more significant than the capillary transport at lower levels of relative humidity is defined as:

$$\delta_p=\frac{\delta}{\mu}, \qquad (5)$$

where

δ is the water vapor permeability in air,

μ is the water vapor diffusion resistance factor.

4.1. Evolution of moisture content

The calibration procedure of the model for moisture transport was complicated by the fact that the evolution moisture content was unknown during the first 408 days of drying when the short companion specimen was cut from the beam, which was then used to measure vertical deflection. For this reason, the calibration can be based only on the moisture balance during the three wetting and drying cycles and the final stage when the companion specimens were immersed in water until their weight stabilized.

The best agreement was obtained with the bilinear sorption isotherm shown in Figure 4 and parameters $A=0.85\,\mathrm{kg\,m^{-2}\,day^{-0.5}}$ and $\mu=250$. It should be noted that the measured data were adjusted to compensate for the rather high content of macropores estimated as 10 %. The three sizes of companion specimens were used for calibration, but a higher weight was given to the smallest size 100 mm (Figure 7) as it was represented by three samples. Compared to the blind prediction, the rate of moisture uptake became significantly accelerated with the Künzel model.

Several snapshots of the graphical postprocessing showing the distribution of relative humidity over the symmetric half of the cross-section with height of 100 mm is shown in Figure 8. The state at the beginning and end of the first wetting cycle is shown in the first two pictures, the red color corresponds to the relative humidity 100 % and the blue color to 45 %. Initially, the relative humidity profile is extremely non-linear and the progress of wetting is very fast. At the end of the wetting cycle, the bottom half of the 100 mm cross-section is almost saturated. The wetting process is much more dominant than drying, the relative humidity has risen to $\approx 70\,\%$ even in the vicinity of the drying surfaces. At the end of the first drying cycle the distribution of relative humidity changes to nicely symmetric with $\approx 65\,\%$ in the core.

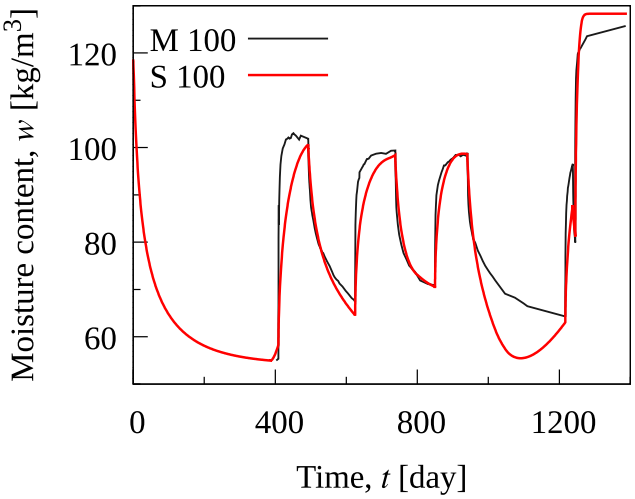

FIGURE 7. Evolution of the average moisture content of the accompanying prism with height of 100 mm. Response of the calibrated model is shown in red, measurement in grey.

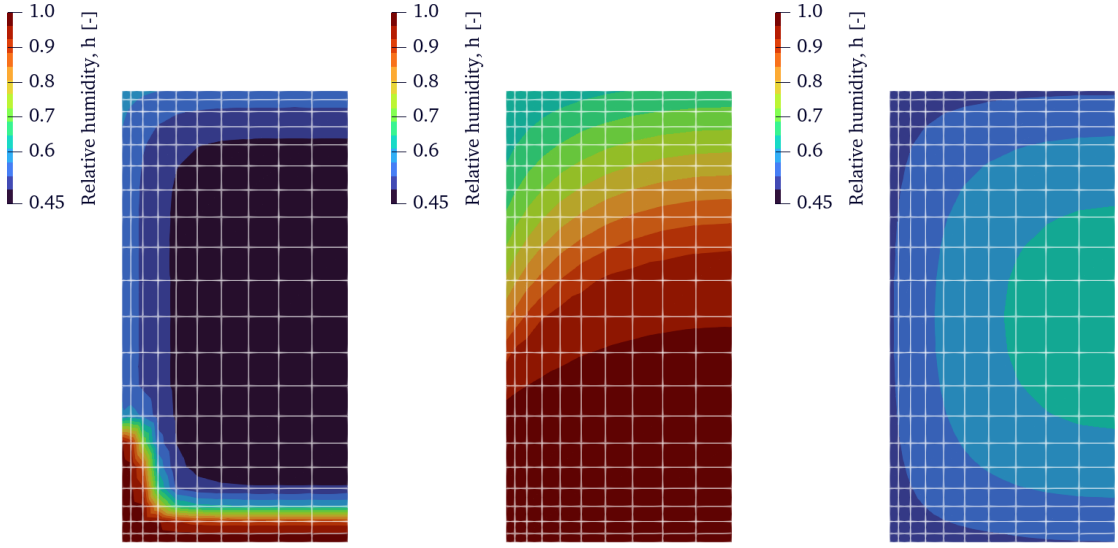

(A). 1st day of wetting. (B). 80th day of wetting. (C). 130th day of drying.

FIGURE 8. Distribution of relative humidity over a the symmetric half of a cross-section (height = 100 mm).

4.2. MECHANICAL RESPONSE

Several modifications of the MPS model for concrete creep were used to compute the response induced by the changing moisture field and by the sustained loading produced by the self-weight. The objective of this study was to identify the governing mechanisms responsible for the behavior observed in the experiments. A detailed discussion can be found in [9].

Graphical postprocessing of the results obtained with the model previously used in the blind prediction shown in Figure 9 illustrates the magnitude of normal stresses in the axial direction of the beam that develop as a response to changing moisture field. The black areas indicate surprisingly high compressive stresses exceeding 8 MPa produced by restrained swelling strain shortly after exposure to wetting, while the gray color shows regions where the tensile stress has exceeded the uniaxial tensile strength 3.38 MPa. Such stresses are produced only shortly after the onset of drying/wetting cycles when the distribution of eigenstrain is extremely nonlinear and the tensile stresses have not been relieved by relaxation. On the basis of these results, it can be concluded that creep can be treated as linear, but the incorporation of a softening behavior in tension is essential.

The evolution of the mid-span deflection obtained with the MPS model with tensile damage extension is shown in Figure 10. The Figure clearly shows that the acceleration in moisture transport has led to a significant acceleration in deflection rate, which is desired for the wetting phase but unintended for all drying phases. In the wetting phases, the computed response for beams with 150 mm and 200 mm height (shown in blue and green lines) is realistic, but the computed deflections reach only approx. $\frac{2}{3}$ of the experimental values. On the other hand, the maximum values for the smallest beam with 100 mm cross section (red line in Figure 10) are correct, but premature equilibra-

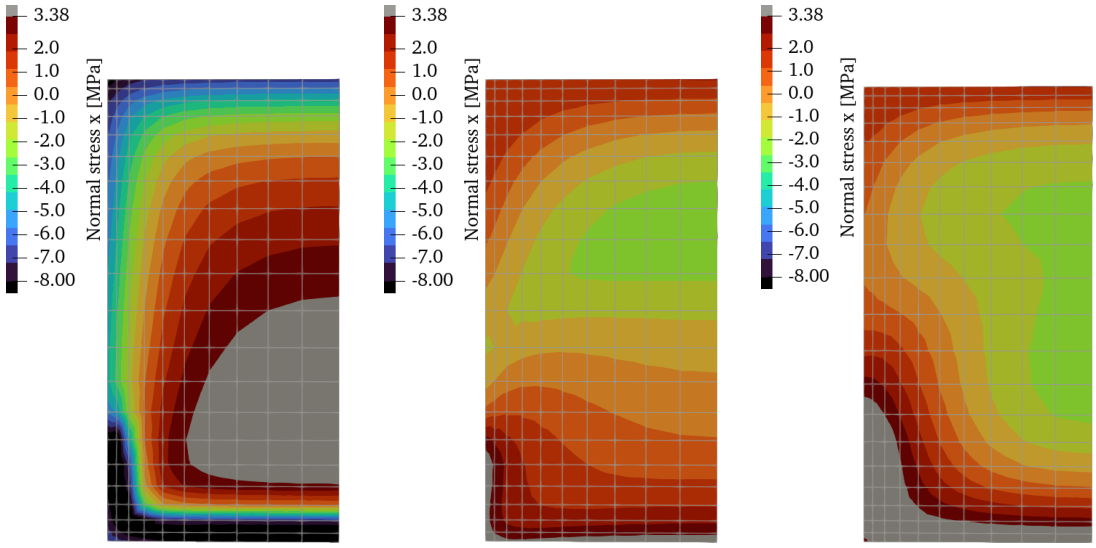

(A). 1st day of wetting. (B). 80th day of wetting. (C). 130th day of drying.

Figure 9. Distribution of normal stress in the axial direction over a the symmetric half of a cross-section at the midspan (height = 100 mm). The gray areas highlight the region where the tensile strength of concrete has been exceeded.

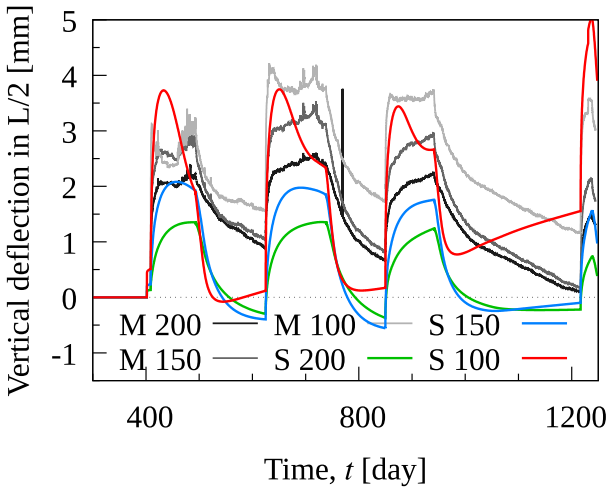

Figure 10. Evolution of vertical mid-span deflection of beams in the experiment (grey scale) and in the calibrated model (colors). The numbers in the legend denote the height of the beams.

tion of the moisture profile has caused an too early decrease in deflection which is not observed in the experiment until the onset of drying.

The rate of the structural response to drying is grossly overestimated. In the experiments, the deflection gradually decreases and would have continued if it had not been terminated by another wetting cycle. Although it is not apparent from the computed results in Figure 10, the contribution to tensile damage is substantial, without it the deflection at the end of the wetting cycles would have been much smaller (negative), which is a consequence of unrealistic creep strains triggered by moisture changes.

5. Conclusion

This paper investigated the influence of partial wetting and drying cycles on the mechanical response of plain concrete beams. The study has shown that a crucial element is a correct description of a moisture transport and that the constitutive model in the subsequent structural analysis is secondary.

The results of the blind predictions demonstrated that the widely used Bažant-Najjar model for transport cannot accurately capture the evolution of the moisture content when the concrete is in direct contact with water. Despite that, the prediction of the structural response which was driven by the (incorrect) moisture field was quite realistic both qualitatively and quantitatively.

Replacing the constitutive model for moisture transport and incorporating the bilinear sorption isotherm has significantly improved the agreement with the measured moisture balance. Despite the effort to calibrate the MPS model and introduce several improvements, the response was similar or worse to that of the blind prediction.

Based on the experimental and numerical results, the following statements can be formulated:

(1.) The influence of tensile damage is significant and cannot be ignored in the analysis.

(2.) At the onset of wetting, damage develops in the core area of the cross section occurring as a result of the expansion of the surface layer of the cross section. This effect increases with decreasing height of the cross section.

(3.) The extent and depth of tensile cracking that develops after sudden exposure to drying increases with cross-sectional height.

Acknowledgements

The authors gratefully acknowledge financial support from the Czech Science Foundation (GA ČR), project number 21-03118S, and from the Grant Agency of the Czech Technical University in Prague, project number SGS23/032/OHK1/1T/11.

References

[1] P. Li, S. He. Effects of variable humidity on the creep behavior of concrete and the long-term deflection of RC beams. *Advances in Civil Engineering* **2018**(1):8301971, 2018. https://doi.org/10.1155/2018/8301971

[2] H. Cagnon, T. Vidal, A. Sellier, et al. Drying creep in cyclic humidity conditions. *Cement and Concrete Research* **76**:91–97, 2015. https://doi.org/10.1016/j.cemconres.2015.05.015

[3] L. Vandewalle. Concrete creep and shrinkage at cyclic ambient conditions. *Cement and Concrete Composites* **22**(3):201–208, 2000. https://doi.org/10.1016/S0958-9465(00)00004-4

[4] G. Pickett. The effect of change in moisture-content on the creep of concrete under a sustained load. In *Journal Proceedings of the American Concrete Institute*, vol. 38, pp. 333–356. 1942. https://doi.org/10.14359/8607

[5] Y. Song, Q. Wu, F. Agostini, et al. Concrete shrinkage and creep under drying/wetting cycles. *Cement and Concrete Research* **140**:106308, 2021. https://doi.org/10.1016/j.cemconres.2020.106308

[6] S. Asamoto, A. Ohtsuka, Y. Kuwahara, C. Miura. Study on effects of solar radiation and rain on shrinkage, shrinkage cracking and creep of concrete. *Cement and Concrete Research* **41**(6):590–601, 2011. https://doi.org/10.1016/j.cemconres.2011.03.003

[7] R. L'Hermite, M. Mamillan. Nouveaux résultats de recherches sur la déformation et la rupture du betón [In French; New research results on deformation and failure of concrete]. *Annales de L'Institut Technique du Batiment et des Travaux Publics* **18**(207):325–359, 1965.

[8] L. Dohnalová, P. Havlásek, V. Šmilauer. Behavior of predried mature concrete beams subject to partial wetting and drying cycles. In *Acta Polytechnica CTU Proceedings*, vol. 34, pp. 1–5. 2022. https://doi.org/10.14311/APP.2022.34.0001

[9] Štěpán Krátký. *Chování betonových nosníků vystavených cyklům částečného namáčení a vysychání: numerické modelování a experiment [In Czech; Behavior of concrete beams subject to partial wetting and drying cycles: numerical modeling and experiment].* Master's thesis, Czech Technical University in Prague, 2023.

[10] B. Patzák. OOFEM home page, 2000. [2023-01-01]. http://www.oofem.org

[11] Z. P. Bažant, L. J. Najjar. Nonlinear water diffusion in nonsaturated concrete. *Materials and Structures* **5**(1):3–20, 1972. https://doi.org/10.1007/BF02479073

[12] Fédération Internationale du Béton. *Model Code 2010 – Final draft, Volume 2.* No. 66 in fib Bulletin. 2012. ISBN 978-2-88394-106-9.

[13] Z. P. Bažant, A. B. Hauggaard, S. Baweja, F.-J. Ulm. Microprestress-solidification theory for concrete creep. I: Aging and drying effects. *Journal of Engineering Mechanics* **123**(11):1188–1194, 1997. https://doi.org/10.1061/(ASCE)0733-9399(1997)123:11(1188)

[14] P. Havlásek. *Creep and shrinkage of concrete subjected to variable environmental conditions.* Ph.D. thesis, Czech Technical University in Prague, 2014.

[15] Z. P. Bažant, S. Baweja. Creep and shrinkage prediction model for analysis and design of concrete structures: Model B3. In *Adam Neville Symposium: Creep and Shrinkage – Structural Design Effects*. 2000.

[16] H. M. Künzel. *Simultaneous heat and moisture transport in building components: One- and two-dimensional calculation using simple parameters.* Ph.D. thesis, University of Stuttgart, 1995.